4.5 Microstrip antenna

Advanced theory

In this paragraph, two-dimensional moment analysis of a patch antenna is presented. In a fact, the approach from par. 4.4 is extended for another dimension.

As already said, electric field intensity has to be expressed as a function of currents and charges over cells. For that purpose, vector potential **A** and scalar potential φ are used. Moreover, the positive convention $\exp(+jkr)$ is considered

$$\mathbf{E} = -j\omega\mu\mathbf{A} - \nabla\varphi. \qquad (4.5B.1)$$

Vector potential **A** and scalar potential φ of elementary planar currents and charges physically represent contributions of sources to the electric field in a given point.

From the mathematical point of view, potentials are the solution of Sommersfeld integrals. For simple situations, potentials can be composed on the basis of the physical point of view. This approach is used even here.

Assume a two-dimensional antenna element over the ground plane (fig. **4.5B.1**). Relative permittivity of the dielectrics is considered (for this moment) to be one, and contribution of an elementary current facet and charge one in the position **r'** to the intensity in **r** is computed. Using Coulomb (resp. Biot-Savart) low and respecting influence of ground plane (mirror principle), we get

$$\mathbf{A}(\mathbf{r}) = \frac{\mu_0}{4\pi}\left[\frac{\exp(-jkr_0)}{r_0} - \frac{\exp(-jkr_1)}{r_1}\right]dr',$$

$$\varphi(\mathbf{r}) = \frac{1}{4\pi\varepsilon_0}\left[\frac{\exp(-jkr_0)}{r_0} - \frac{\exp(-jkr_1)}{r_1}\right]dr',$$

where the distances r_0 and r_1 are

$$r_0 = \sqrt{(x-x')^2 + (y-y')^2},$$

$$r_1 = \sqrt{(x-x')^2 + (y-y')^2 + (2h)^2}.$$

Fig. 4.5B.1 *Coordinate system for computing contributions of elementary current (resp. charge) elements*

Here $\mathbf{r} = (x, y)$, $\mathbf{r'} = (x', y')$ and h denotes the height of the substrate.

Including the influence of the dielectrics is more complicated. The physical notion tells us that wave can propagate to the observation point **r** by the infinite number of paths:

$$\varphi(\mathbf{r}) = \frac{1-\eta}{4\pi\varepsilon}\left[\frac{\exp(-jk_0 r_0)}{r_0} - (1+\eta)\sum_{i=1}^{\infty}\frac{(-\eta)^{i-1}\exp(-jk_0 r_i)}{r_i}\right],$$

where

$$\eta = \frac{\varepsilon_r - 1}{\varepsilon_r + 1}, \qquad r_i = \sqrt{x^2 + y^2 + (2ih)^2}$$

and ε_r is relative permittivity of the substrate.

Vector potential **A** stays unchanged.

In the case of sources of finite dimension (rectangular cells), the contribution is expressed in integral way

$$\mathbf{A}(\mathbf{r}) = \iint_{p\check{r}es\,plochu\,bu\check{n}ky} \mathbf{G}_A(|\mathbf{r}-\mathbf{r'}|)\mathbf{J}(\mathbf{r'})\,dS', \qquad (4.5B.2)$$

$$\varphi(\mathbf{r}) = \iint_{p\check{r}es\,plochu\,bu\check{n}ky} \mathbf{G}_q(|\mathbf{r}-\mathbf{r'}|)q(\mathbf{r'})\,dS', \qquad (4.5B.3)$$

where $\mathbf{G}_A$ and $\mathbf{G}_q$ are Green functions for magnetic potential and electric one, σ is charge density.

Now, eqn. (4.5B.2) is discretized. In order to meet this task, a contribution of an arbitrary current (charge) cell to the potential in the center of another cell has to be expressed. Therefore, we denote

$$m_{ij}^{Ax} = \iint_{p\check{r}es\,plochu\,i-t\acute{e}bu\check{n}ky} G_{xx}^A(|\mathbf{r}_j-\mathbf{r'}|)J_x(\mathbf{r'})\,dS', \qquad (4.5B.4a)$$

$$m_{ij}^{Ay} = \iint_{p\check{r}es\,plochu\,i-t\acute{e}bu\check{n}ky} G_{yy}^A(|\mathbf{r}_j-\mathbf{r'}|)J_y(\mathbf{r'})\,dS', \qquad (4.5B.4b)$$
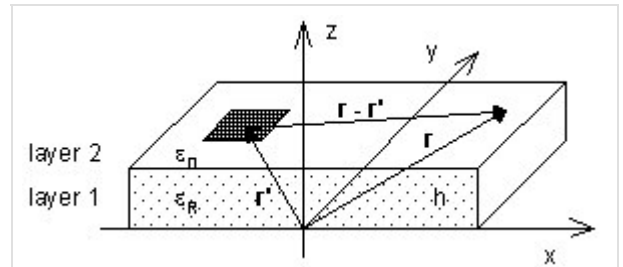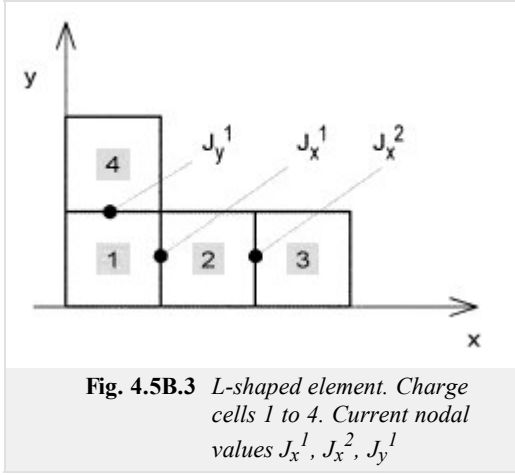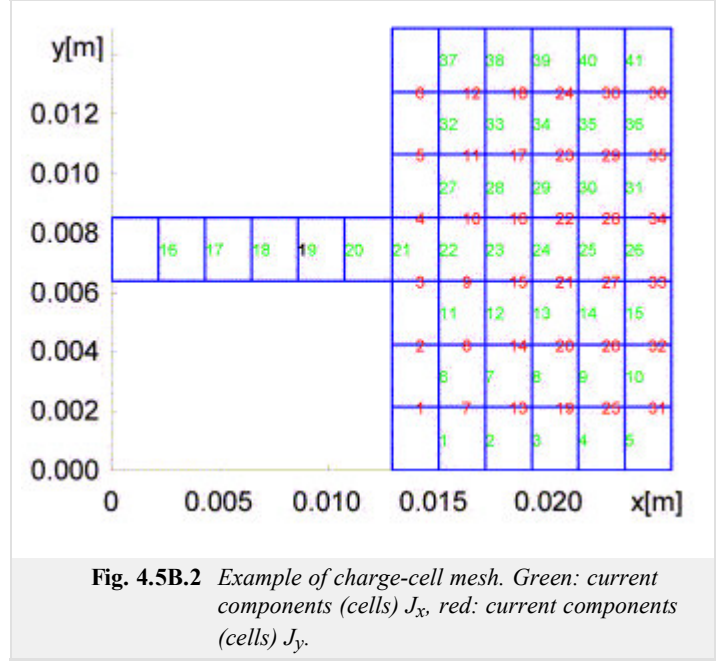
$$m_{ij}^{\varphi} = \iint_{p\check{r}es\,plochui-t\acute{e}bu\check{n}ky} G^q\left(|\mathbf{r}_j - \mathbf{r}'|\right)\sigma(\mathbf{r}')\,dS'. \qquad (4.5B.5)$$

Expression m_{ij}^{Ax} tells how j-th current cell for x-component contributes to vector potential in the center of i-th cell. Similar meaning is observed at m_{ij}^{Ay} for J_y and at m_{ij}^{φ} for scalar potential. As shown in the layer A, meshes of current cells and charge ones are mutually shifted for one half of a cell, and hence, a different numbering is used. Moreover, we independently number current cells for x-component and y-component. This fact is illustrated by numbering in fig. **4.5B.2**, which corresponds to the structure in fig. **4.5A.3**.

Fig. 4.5B.2 *Example of charge-cell mesh. Green: current components (cells) J_x, red: current components (cells) J_y.*

Composing equations for unknown current

Fig. 4.5B.3 *L-shaped element. Charge cells 1 to 4. Current nodal values $J_x{}^1$, $J_x{}^2$, $J_y{}^1$*

distribution, we have to know a function describing contributions between two arbitrary cells (of the same type). Due to the limited space, we do not describe this function here. We state only that all the contributions are evaluated at the beginning of the program. Moreover, several contributions repeat (e.g., cells 1 and 2 for the component J_x are of the same contribution as cells 3 and 4). The mutual contributions are stored in a moment table (matrix). Calling the function, a contribution on a respective position of the table is read.

Now, the set of equations can be composed. We do not introduce a general relation, but a given simple situation is described. Fig. **4.5B.3** contains a L-shaped antenna element, consisting of four charge cells and three current cells (two of them are related to J_x, one of them to J_y).

Next, equations for $E_1{}^x$ are built:

$$E_1^x = -j\omega \sum_{j=1}^{3} m_{1j}^{Ax} - \frac{1}{\Delta}\left[-\frac{j}{\omega}\frac{J_1^x - 0}{\Delta x} + \frac{J_1^y - 0}{\Delta y}\left(m_{21}^{\varphi} - m_{11}^{\varphi}\right) - \frac{j}{\omega}\frac{0 - J_2^x}{\Delta x} + \frac{0 - 0}{\Delta y}\left(m_{23}^{\varphi} - m_{13}^{\varphi}\right) - \frac{j}{\omega}\frac{0 - 0}{\Delta x} + \frac{0 - J_2^y}{\Delta y}\left(m_{24}^{\varphi} - m_{14}^{\varphi}\right) \right].$$

The first term represents the contribution of all current cells to the current cell $J_x{}^1$. The second term represents the contribution of charge cells; expression $\{\}/\Delta x$ denotes replacing the derivative $\partial\varphi/\partial x$ by the central difference (see par. 4.1). Brackets contain three terms since there are four charge cells. E.g., the first term represents the contribution of the first charge cell to the center of the second cell minus the contribution of the first charge cell to the center of the first cell. I.e., the first index at m denotes the center of the observation charge cell, where the contribution is computed, and the second index denotes the source cell. Charge in each cell is evaluated using nodal current densities and exploiting continuity equation

$$\nabla \cdot \mathbf{J} = -j\omega\sigma, \qquad (4.5B.6)$$

where J[A/m] and σ[C/m^2] are current density and charge density.

Similarly, equations for $E_2{}^x$ and $E_1{}^y$ can be composed. Next, we turn our attention to feeding the structure.
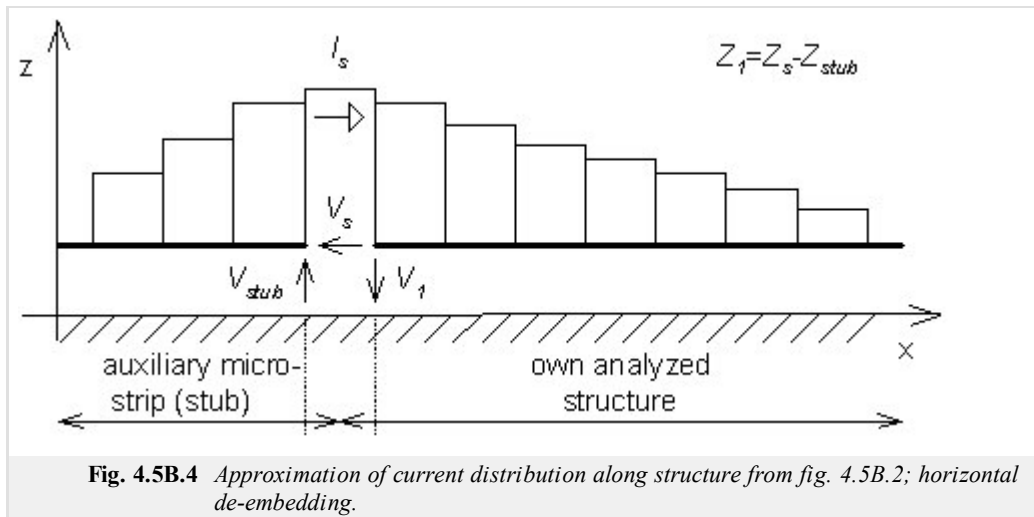
Plane wave feeding is the simplest way of feeding (see par. 4.4). For each current cell, we substitute $E_x = -E_x{}^I$ and $E_y = -E_y{}^I$, where $E_x{}^I$ and $E_y{}^I$ represent components of incident wave. In our situation, the antenna is assumed to be fed by a voltage source, which is connected between the analyzed structure and an auxiliary microstrip (the incident wave is not considered). In detail, the situation from fig. **4.5B.2** is depicted in fig. **4.5B.4**.

In the position, where 1 denoted the input port in fig. **4.5B.2**, a voltage source of a voltage V_S is considered. The source supplies the structure by the current I_S. One pole of the source is connected to the analyzed structure, the second pole is connected to the auxiliary microstrip (*stub*), which represents a certain impedance Z_{stub} related to ground. Input impedance Z_1 is then given by the relation

$$Z_1 = Z_S - Z_{stub}, \qquad (4.5B.7)$$

where the impedance Z_S is determined as the ratio of the voltage V_S (its value is eligible) and the current I_S. The impedance Z_{stub} is computed

analytically as $-Z_0 \cot(\beta\, l_{stub})$.

Fig. 4.5B.4 *Approximation of current distribution along structure from fig. 4.5B.2; horizontal de-embedding.*

If impedance is computed by the above-described way, the result does not correspond to the reality because influence of edge capacitances is not considered (see fig. **4.5B.5**).

Fig. 4.5B.5 *Edge capacitances*
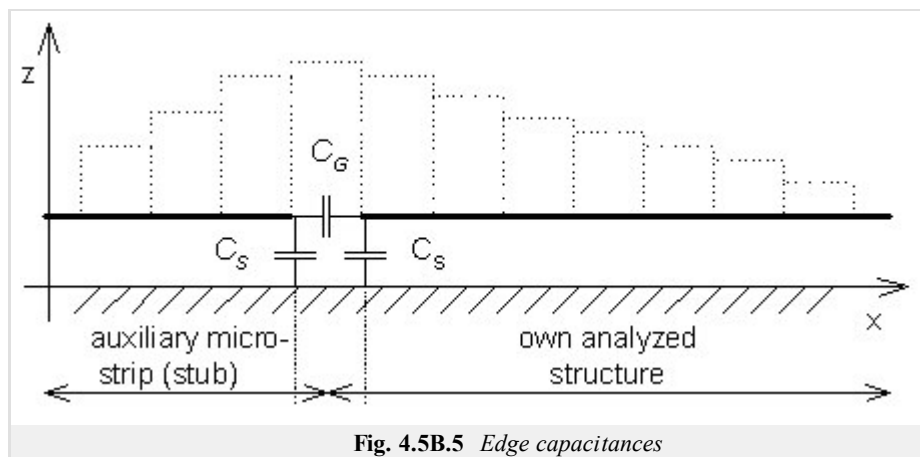
Respecting capacitances, the impedance Z_{stub} has to be added in parallel to $Z_S = 1/j\omega\, C_S$ (C_S is not open-end capacitance, but it is smaller). That way, we get $Z_{stub}' = Z_{stub} \parallel Z_S$. Capacitance C_G is already included in the impedance Z_S and computing impedance $Z_1{'} = Z_S - Z_{stub}{'}$, we have to subtract Z_S. The final impedance is $Z_1{''} = Z_1{'}\, Z_S\, /\, (Z_S - Z_1{'})$.

Finally, we give a note about feeding the structure.

We can assume the structure to be fed by a voltage source connected between the microstrip and ground. This approach causes the direct computation of input impedance from the voltage and the current to provide results, which differ from the measured value. The reason of this difference is hidden in the fact that long cables are used for measuring, and therefore, the TEM wave (forward one, backward one) is present in the point of interest. If feeding is implemented by the above-described source connected between the microstrip and ground (localized feeding), then field distribution at the positive pole does not correspond to the field caused by TEM waves, but end effect influences results. In practical life, the result of localized feeding has to be transformed to the long-cable feeding (vertical de-embedding). The current standing wave has to be de-composed to the forward wave and the backward one. De-composition is not performed at the source port, but is shifted to the right. If both the waves are known, then reflection coefficient can be evaluated at the position of measurement. Then, the phase of reflection coefficient is shifted to the computation position.

The set of equations for unknown nodal values was built respecting physical principles. Now, the mathematical approach, which corresponds to the above-described notions, is given:

- Current density is approximated in terms of basic functions

$$J_X(x,\, y) = \sum_{n=1}^{N_X} J_{X_n} B_{X_n} \qquad J_Y(x,\, y) = \sum_{n=1}^{N_y} J_{Y_n} B_{Y_n}$$

In our approach piecewise constant basis functions are used. As another possibility, *rooftops* can be used (linear in the first direction, constant in the second direction).

- Integral expression of potentials based on Green functions is substituted to (4.5B.1)

$$\left\{ -j\omega \iint_{\Omega} \mathbf{G}_A(x-x',\, y-y') \mathbf{J}(x',\, y')\, dx'dy' \right\} + \left\{ -\nabla \left[\iint_{\Omega} \mathbf{G}_q(x-x',\, y-y')\rho(x',\, y')\, dx'dy' \right] \right\} + \mathbf{E}^I = 0.$$

Here, W denotes the metallic area and E^I is intensity of incident wave. In most cases, the structure is fed via microwave ports and E^I is zero. Analyzing selective surfaces e.g., plane-wave feeding is assumed.

Charge is substituted from continuity equation and current density is expressed as a combination of basis functions. That way, we obtain

$$\tilde{J}_x^{(n)}(x,\, y) = \sum_{nx=1}^{N_x} J_x^{(nx)} \Pi^{(nx)}(x,\, y)$$

$$\left\{ -\frac{1}{j\omega} \frac{\partial}{\partial x} \iint_{\Omega} G^q(x-x',\, y-y') \left[\frac{\partial}{\partial x} \sum_{n=1}^{N_x} J_{X_n}(x',\, y') + \frac{\partial}{\partial y} \sum_{n=1}^{N_y} J_{Y_n}(x',\, y') \right] dx'dy' \right\} + E_X^I = 0,$$

$$\left\{ +j\omega \iint_{\Omega} \mathbf{G}_{yy}^A(x-x',\, y-y') \sum_{n=1}^{N_y} J_{Y_n}(x',\, y')\, dx'dy' \right\} -$$

$$\left\{ -\frac{1}{j\omega} \frac{\partial}{\partial y} \iint_{\Omega} G^q(x-x',\, y-y') \left[\frac{\partial}{\partial x} \sum_{n=1}^{N_x} J_{X_n}(x',\, y') + \frac{\partial}{\partial y} \sum_{n=1}^{N_y} J_{Y_n}(x',\, y') \right] dx'dy' \right\} + E_Y^I = 0.$$

- Exploiting Galerkin method, current approximation error is minimized. Then, the following set of equations is obtained:

$$\sum_n J_n^X \left\{ \langle T_{xm},\, G_{xx}^A * B_{xn} \rangle + \frac{1}{\omega^2} \langle T_{xm},\, \frac{\partial}{\partial x} \left[G_q * \frac{\partial}{\partial x} B_{X_n} \right] \rangle \right\} + \sum_n J_n^Y \left\{ \frac{1}{\omega^2} \langle T_{xm},\, \frac{\partial}{\partial x} \left[G_q * \frac{\partial}{\partial y} B_{yn} \right] \rangle \right\} = 0,$$

$$\sum_n J_n^X \left\{ \langle T_{ym},\, G_{yy}^A * B_{yn} \rangle + \frac{1}{\omega^2} \langle T_{ym},\, \frac{\partial}{\partial y} \left[G_q * \frac{\partial}{\partial y} B_{yn} \right] \rangle \right\} + \sum_n J_n^X \left\{ \frac{1}{\omega^2} \langle T_{ym},\, \frac{\partial}{\partial y} \left[G_q * \frac{\partial}{\partial x} B_{xn} \right] \rangle \right\} = 0$$

.

Inner integrals are of convolution nature, and therefore, they are denoted by asterisk. Outer integrals are of correlation nature, and hence, they are denoted by brackets $\diamond$. The symbol T denotes weighting functions (in Galerkin method, they are identical with basis functions).

From the mathematical point of view, Dirac pulses play the role of weighting functions in our formulation of moment method. This approach is called collocation method.

- All the integrals are efficiently evaluated and set of equations is composed. Solving it, unknown nodal values of current density are obtained.

- On the basis of known current distribution, other antenna parameters can be computed (reflection coefficient at a given port, input impedance, etc.).

In the layer C, the patch antenna analysis by the moment method is illustrated by an example.